ABRASIVE WEAR IN PUMPS– A TRIBOMETRIC APPROACH TO IMPROVE PUMP LIFE

by
Gerhard Vetter
Professor
Ralph Kießling
and
Wolfgang Wirth
Research Engineer
University of Erlangen-Nuremberg
Erlangen, Germany

Gerhard Vetter obtained his Dipl. Ing. degree (Mechanical Engineering) at Technische Universität Karlsruhe, Germany. After some years as a Research Engineer in turbomachinery at the same university, he joined Lewa, Leonberg (Germany) as head of the Research and Development Department. He became Chief Engineer and, in 1970, Technical Managing Director. In 1981, he accepted a chair (professorship) for Apparatus and Chemical Machinery at the University of Erlangen-Nuremberg. He is a corresponding member of the International Pump User's Symposuim Advisory Committee.

Prof. Vetter has dedicated more than 25 years to research, development and design of pumps and metering equipment. He has been one of the pioneers in diaphragm pumps development. Many papers, patents, and contributions to textbooks, some dealing with basics like cavitation, fatigue, pulsation, vibrations, abrasive wear and metering accuracy, have established his reputation as a pump specialist. The well equipped laboratory at University of Erlangen-Nuremberg performs research work on pump and metering subjects.

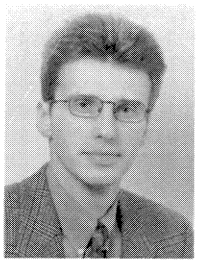

Ralph Kießling studied in the Department of Chemical Engineering at the University Erlangen-Nuremberg, Germany. After receiving his Dipl.-Ing. degree in 1992, he joined the Institute of Apparatus and Chemical Machinery at the same University. His research subjects were hydroabrasive wear in rotary positive displacement and centrifugal pumps, especially in clearance seals. On this topic he prepared a doctoral thesis in 1994 (Dr.-Ing. degree).

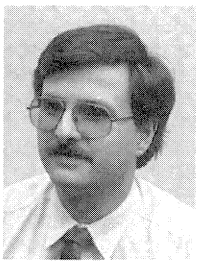

Wolfgang Wirth obtained his Dipl.-Ing. Univ. degree (Chemical Engineering) at the university of Erlangen-Nuremberg, Germany in 1986, and subsequently joined the Institute of Apparatus and Chemical Machinery at the same institution. As a research engineer, he prepared a thesis about methods for modelling of the hydraulic and tribologic properties of progressing cavity pumps and received his Dr.-Ing. degree in 1993.

ABSTRACT

The reduction of abrasive wear and extension of the endurance of pumps requires a system analysis. Various pump types demonstrate different tribological systems under abrasive wear, which are basically dominated by sliding, jet, and stamping wear types. The morphological approach yields an understanding of why wear attacks have to be considered predominantly.

Chances and limitations for wear and endurance prediction based on tribometric simulation are discussed. As quantitative prediction is not always possible, the method of relative suitability turns out to be a good tool.

As experience shows predominant jet and sliding wear in pumps, these two wear types are discussed closer.

A good example for a tribological system dominated by sliding wear is the progressing cavity pump. Several tribological simulations, including parameter studies are discussed, evaluated, and compared that demonstrate strategies for pump improvements.

Jet wear dominated tribological systems are special clearances in rotary pumps that are discussed with respect to wear phenomena and tribological simulation. Furthermore, methods of wear prediction for centrifugal pumps in general, based on parameter studies with jet tribometers, are explained.

The discussion is ended with an extended analysis of various materials, different steel, and sintered types in solid or layered

along with plastics for application in pumps against hydroabrasive wear, following the method of relative suitability based on tribometric data for jet and sliding wear.

INTRODUCTION

There are many applications for pumps in processing and conveying systems, where suspensions, slurries, or particle contaminated fluids have to be handled. The interaction of abrasives with the pump parts is characteristically for the various pump types, demonstrating at certain locations wear rates by erosion that may cause severe reduction of pump life cycle.

Typical failures are increased clearances at intermeshing sealing parts implementing larger internal leak losses, as is shown in Figures 1 and 2 [1], for the rotor of a progressing cavity and the valve seat of a reciprocating pump [2]. The alteration of the rotor shape with centrifugal pumps, be it surface quality or flow channel geometry in general, is strongly influencing pump performance and function (Figure 3).

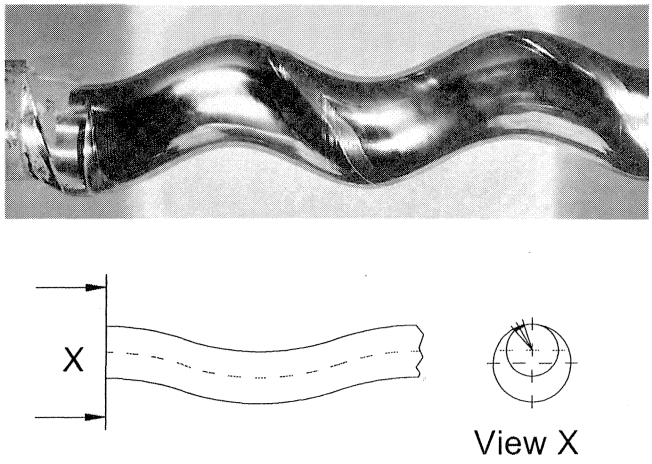

Figure 1. Wear at the Rotor of a Progressing Cavity Pump (Helical Wear Traces).

Abrasive wear which is directly responsible for the reduction of energetic and volumetric efficiency, life cycle time, malfunction, safety and economy has to be avoided by a tribological analysis of the endangered pump locations.

The authors feel that this paper will stimulate the application of systems analysis and tribometry to achieve the extension of pump life cycles.

Basics of Tribometric Simulation

Wear, per definition is the permanent material loss at the surface of pump components by mechanical and combined chemical action, representing not a material but a systems characteristic. The physical wear mechanisms comprise adhesion, abrasion, surface fatigue, tribo oxidation and tribo corrosion effects [3]. In general, tribological systems by superposition of several wear mechanisms demonstrate typical wear types like jet, sliding, rolling, resp. stamping wear.

As an example, the tribological system is shown in Figure 4 of sliding wear, with the system components: the intermeshing components (positions 1 and 2) the fluid (position 3), the particles (position 4) and other characteristics like temperature, chemical and physical fluid, and particle properties. Each pump type demonstrates one or more characteristically tribological systems that have to be analyzed in order to recognize the predominating important parameters on wear.

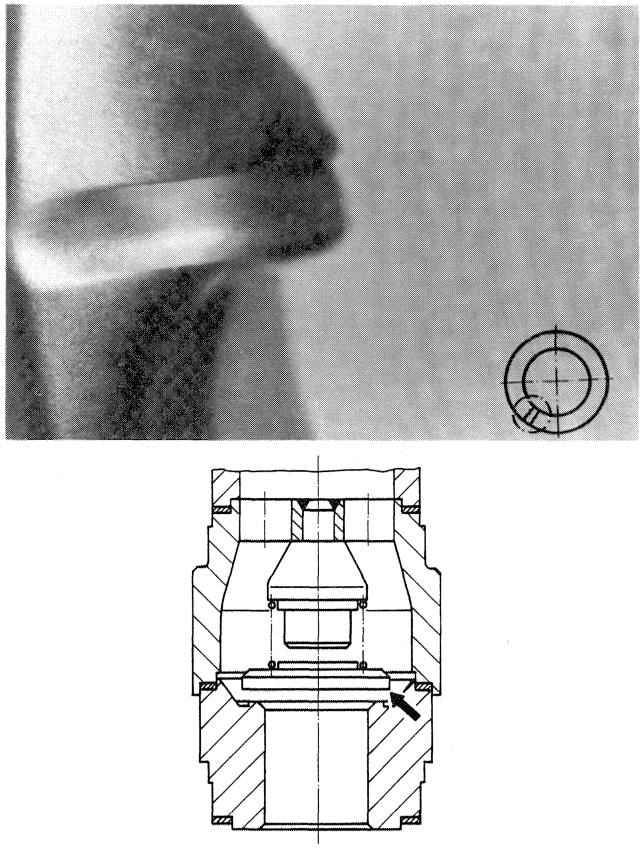

Figure 2. Local Jet Wear Traces at the Metallic Seat of a Reciprocating Pump Check Valve.

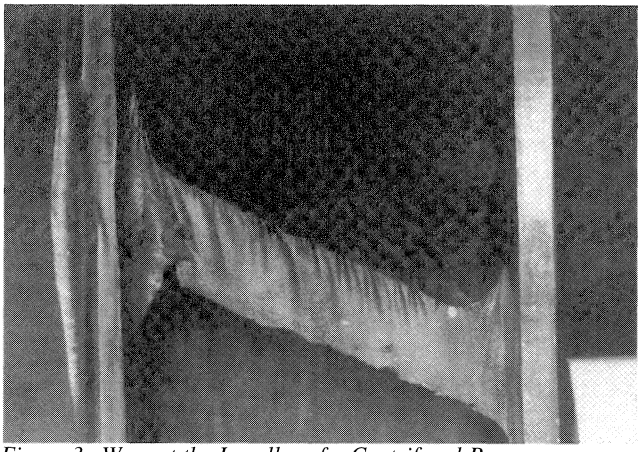

Figure 3. Wear at the Impeller of a Centrifugal Pump.

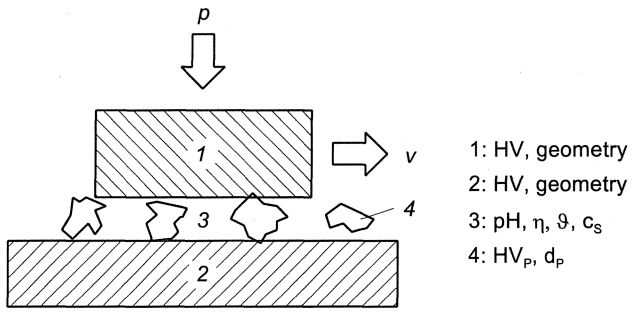

Figure 4. Tribological Sliding Wear System: 1) wear component; 2) wear component; 3) fluid; 4) abrasive particle.

The further explanation will exclusively concentrate on hydroabrasive tribological systems.

The basic idea of tribometric simulation is to analyze the pump with respect to the relevant wear locations, in order to find out the predominantly active tribological systems and methods for their tribometric simulation with flexible and simple test rigs.

Wear Locations

Considering a number of representative pump types (Figure 5) including centrifugal pumps, rotary, and reciprocating displacement pumps shows that hydroabrasive tribological systems in pumps are mainly based on three wear types: jet, sliding, and stamping or rolling wear.

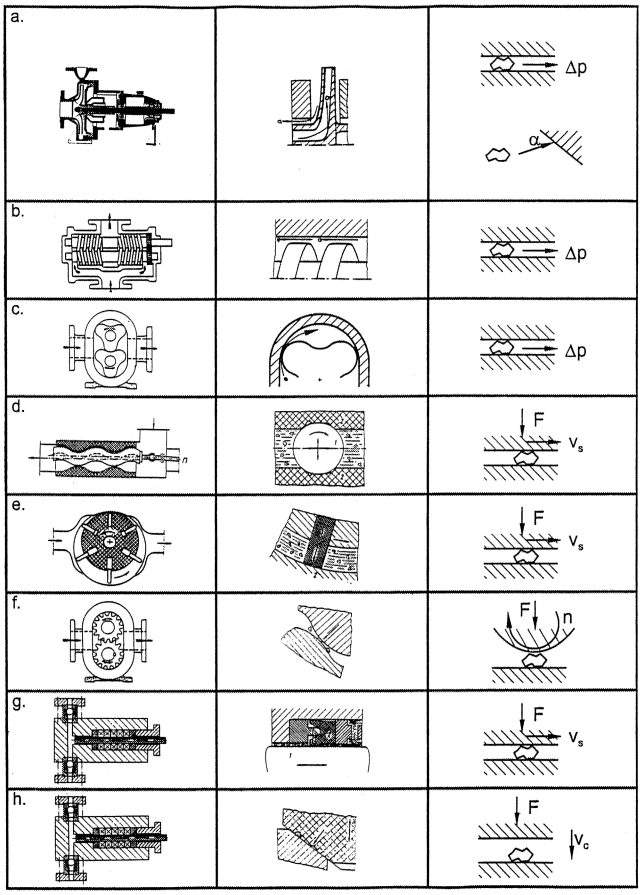

Figure 5. Morphology of Wear Locations for Various Pump Types: a) centrifugal; b) two screw; c) three lobe d) progressing cavity; e) sliding vane; f) gear; g) reciprocating (plunger seal); h) reciprocating (check valve).

The hydroabrasive jet wear type is characteristic at all types of flow channels in impellers or housings with or without blades (Figure 5(a)), the particles may move parallel or angular relative to the wearing walls.

A special case of hydroabrasive jet wear is the flow in annular clearance seals where the particles move predominantly parallel to the walls and are typical for all types of rotary pumps, including the displacement types that demonstrate radial and axial clearance like screw, lobe, progressing cavity, or vane features. A good example for these clearance configurations represents the two screw design with external timing gear (Figure 5(b)) that needs three clearances (Figure 6) in order to seal the working chamber. Very similar is the situation in lobe pumps (Figure 5(c)) with external timing gears.

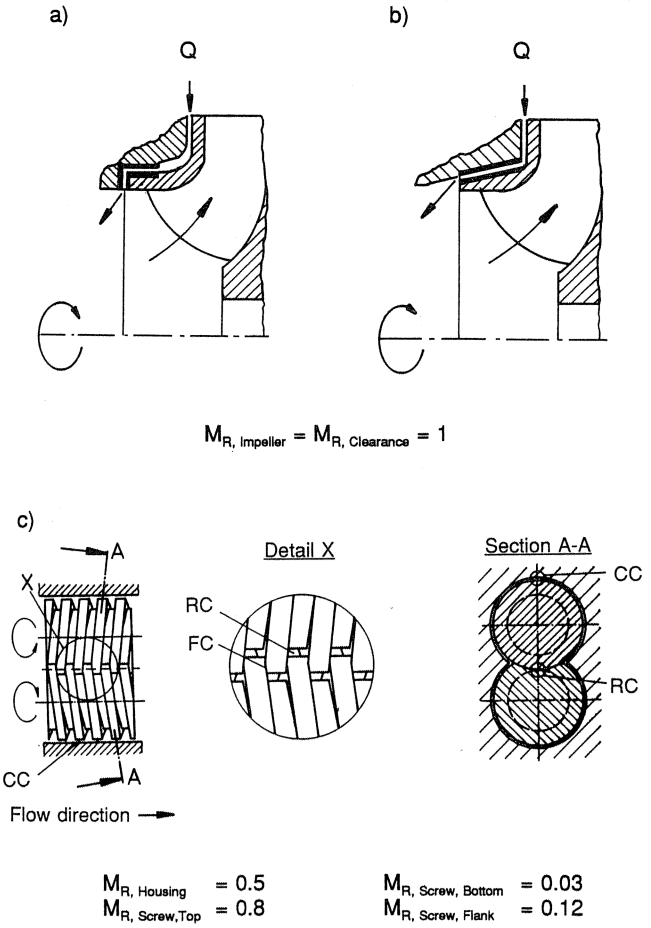

Figure 6. Meshing Ratio (examples): a), b) centrifugal; c) two screw.

The tribological system of rotary displacement pumps with sliding internal sealing lines as demonstrated by single screw (progressing cavity) and sliding vane pumps represents predominantly a sliding wear type where particles are squeezed under relative motion within the sealing zone, depending on their size.

Distinguished differences should be noted: The elastic (elastomer) stator of the single screw pump allows relatively soft embedding of the particles so that there compression forces onto the rotor remain small, large particles being rejected from the sealing area (Figure 5 (d)). This tribological system is very similar to plunger (Figure 5(g)) and valve seals when elastomeric seal elements are applied, except the motion type and direction.

In any case, intermeshing seals represent exclusively sliding wear tribological systems if the leak flow remains very small.

The tribological system of sliding vanes is similar (Figure 5(e)) also to plunger seals as the seal element is permanently compressed and moved relative to the wall, allowing only fine grain particles to enter and rejecting larger ones.

The tribological system of intermeshing and torque transmitting gear pumps (Figure 5(f)) is of the rolling wear type. This is an important difference compared with three lobe pumps with external timing gear, where there is no rolling but jet wear in the intermeshing zone. As particles in the power transmitting intermeshing zone are unavoidably crashed, the tribological system is requiring greater hardness of the gear parts than that of particles as a must.

The tribological system of pump check valves is similar but of the stamping wear type with the same consequences with respect

to hardness except one of the seal parts can be made of elastomeric material (Figure 5(h)).

Characteristic Wear Types

From the morphological study above, yield the three predominantly important wear types for hydroabrasive pump wear: jet, sliding, rolling, or stamping wear. It should be noted however, that normally different wear types act in a superimposed manner or during operation the tribological system may change its character.

It requires empirical experience with a certain feature of pump in order to select a suitable wear simulation method.

Some detailed considerations should be noted:

Meshing ratio. The various tribological systems in pumps show wear locations that are engaged permanently or on a part time basis (Figure 6). The meshing ratio M_R is defined as

$$M_R = \frac{t_M}{t_{tot}} \qquad (1)$$

where t_M is the meshing time of the tribological system, and t_{tot} is the total relevant time period.

For clearances and flow ducts in centrifugal pumps, the meshing ratio yields $M_R = 1$ (Figure 6(a)). The meshing ratios for the three clearances of a two screw pump for example yield differently, but $M_R < 1$.

This finding shows that for that special pump feature, the locations with the highest meshing ratio should receive most attention, because the physical wear type is very similar for all locations (Figure 6(b)).

All pump types demonstrate characteristic meshing ratios. For progressing cavity pumps the meshing ratio changes strongly with the angular position at the rotor yielding predominantly local wear attack along a helical zone (Figure 1).

Particle motion. The penetration of particles into clearances or sliding zones needs closer consideration (Figure 7). For sliding wear systems, the clearance under the acting compression is determined by the force balance and the particle sizes that may yield a tight meshing without, or a more or less leaking clearance system with jet wear.

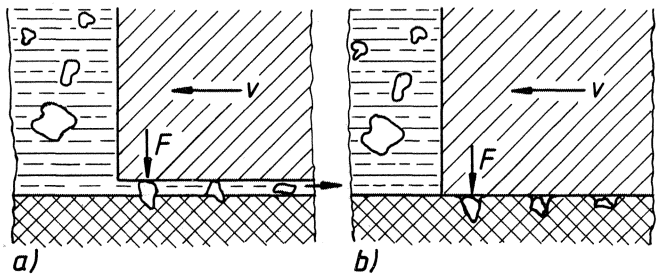

Figure 7. Particle Access in Sliding Wear Tribological Systems: a) clearance, leakage; b) no clearance, no leakage.

As a result, it seems rather difficult to predict what particle collective exists in the meshing zone, explaining basic difficulties with efficient tribometric simulation of sliding wear systems.

For jet wear systems in large flow channels (particle size d_P « flow channel dimension), flow angle and speed of the particles are dominant parameters that can be well simulated, but it is very difficult for practical purposes to understand the real particle path with respect to angle and kinetic energy (Figure 8(a)).

It will be shown in further chapters that parallel and angular particle motion generate very different wear rates, orthogonal motion representing, for most materials, the worst condition.

Clearances with definite dimensions tend to separate the particle collective, rejecting too large ones. This separation process may

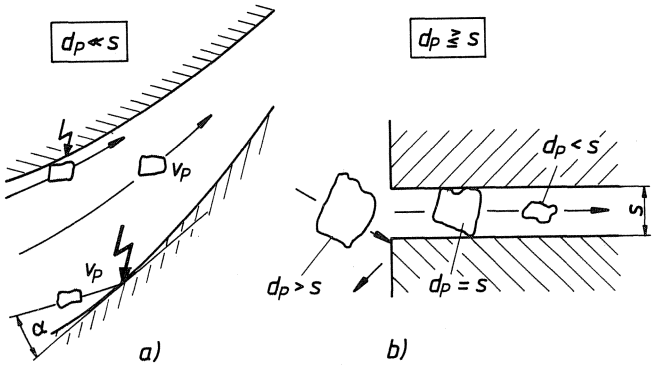

Figure 8. Particle Motion in Jet Wear Tribological Systems.

happen in centrifugal pumps by centrifugal separation effects and is a means to influence what particle sizes arrive at a clearance.

The tribological system turns from mere jet wear to sliding wear resp. score grooving if particle size equals clearance with the consequence of much larger wear rates. The simulation of plain jet wear in clearances is most efficient and quantitative, whereas that of the mixed tribological system with partial score grooving includes a potential of uncertainties.

From these explanations yield strategic approaches to reduce wear by influencing the tribological system itself.

Particle hardness. It will be shown in later sections that the hardness ratio R_H between the attacking particles (HV_P) and wearing surfaces (HV_S) is an outstanding parameter for hydrabrasive wear in general (HV Vicker hardness).

$$R_H = \frac{HV_P}{HV_S} \qquad (2)$$

From many tribological systems, and this is verified for the basic ones (jet, sliding, rolling, stamping) too, wear rates can be reduced best if $R_H < 1$.

For rolling or stamping wear (gear pumps, reciprocating check valves) where particle crashing or grinding with hard pump components (who is stronger?) is unavoidable, a hardness ratio $R_H < 1$ (the smaller the better!) is a must [4].

The quantitative simulation of stamping wear in reciprocating pumps' check valves has been verified. It should be noted that particle access, basically not obstructed, can be in a certain amount influenced by the meshing geometry of valve parts. For stiff and hard valve parts (Figure 9(a)), the remaining clearance is determined by the size of the partly crashed particles at high pressure differentials that yields a very characteristic instability of the tribological system [5] caused by jet wear effects (Figure 2). The strategy to eliminate the instability is to avoid jet wear by one elastomeric valve part (Figure 9(b)) that yields a definite and not superimposed stamping tribological system.

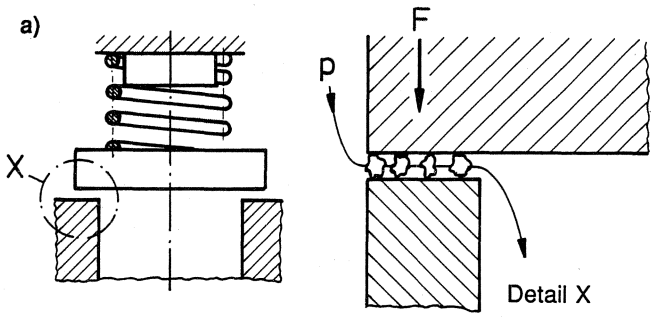

Figure 9. Stamping Wear Features: a) rigid valve parts, jet wear involved; b) one elastic valve part, no jet wear.

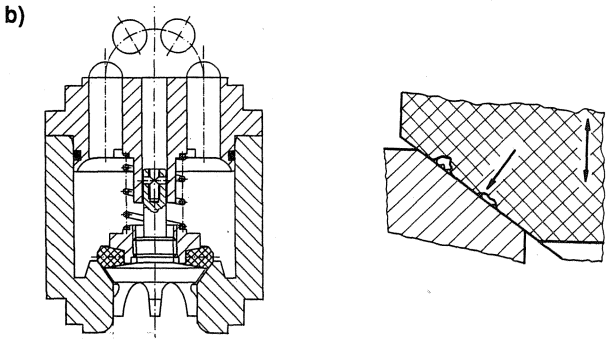

Figure 9.

Tribometric Simulation for Pump Optimization

Since field tests are expensive and time consuming, they are not suitable for extended parameter studies. It is, therefore, advantageous to simulate the tribological system at lower costs and find a wear prediction that may represent the result of a number of iterations.

An example for the more or less precise tribometric wear prediction shows Figure 10, the pump field tests representing the best 'simulation' [1].

Parameter	Pump (Field Test)	Rot./Osc.Tribometer (ROS)	Sliding Tribometer (Miller)
	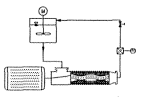	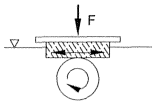	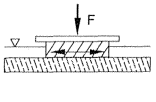
Geometry: abs. Size	++	-	-
rel. Size	++	++	-
Meshing	++	+	-
Kinematics	++	+	-
Function	++	+	-
Materials	++	++	++
Fluid	++	+	+
Quality of Simulation	precise	approx. quantitative	qualitative

Figure 10. Example for Tribological Simulations with Progressing Cavity Pump.

There are tribological systems that allow very efficient simulations (Figure 11(a)), others implement major difficulties so that the method of relative suitability must be applied. This strategy is based on the simulation of the predominant wear types with simple tribometers, in order to find better suitable materials. A wear prediction yields only approximative, and not quantitative.

The method normally starts with the analysis of pump failures (tribological system TS1 (Figure 11(b)). With tribological simulations (several relevant wear types TSI, TSII) and tribometric results (TM 1.4) yields a better suitable material choice.

In the following sections, the potential of tribologically based abrasive wear reduction in pumps with dominating sliding resp. jet wear are described in more detail.

TRIBOSYSTEMS IN SPECIFIC TYPES OF PUMPS

The principles of tribometric simulation described are now explained on selected examples:

- Sliding wear: Progressing cavity pump
- Jet wear: Two-screw pump, resp. centrifugal pump

Tribosystems Predominantly Experiencing Sliding Wear

The progressing cavity pump (Figure 5(d)) represents a typical example of a system predominantly experiencing sliding wear.

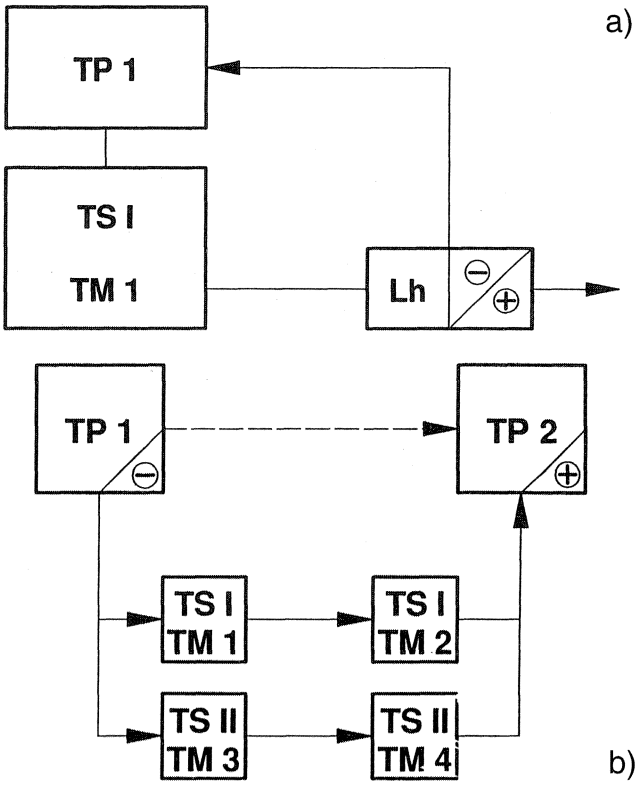

Figure 11. Examples for Wear Prediction: a) quantitative prediction; b) method of relative suitability, T_P = tribosystem pump; T_S = tribometric simulation (= tribometer); TM = tribometric measurement.

Investigations on the wear in the tribosystem 'progressing cavity pump' can be performed without abstraction on a real pump, or by means of tribometers involving various degrees of abstraction [6].

Field Tests on the Actual Pump

While field tests usually require considerable efforts, they permit an optimal acquisition of the mechanisms and processes involved in this type of wear. The relative change in the ratio of the masses m/m_N (m_N = initial mass, m = mass reduced due to wear) is subsequently shown.

The loss of mass represents a direct measure for the geometric reduction of the diameter of the rotor and, accordingly, for the reduction of the interference existing in the pump. The approximate change of the shape of the rotor can be computed comparatively easily from the loss of mass.

Under the conditions selected for the test, only minor jet wear was observed. After the test, the worn rotors showed no wear marks, indicating a gap flow.

A few influential factors are now discussed:

Rotary speed n:

It is convenient to plot wear against total sliding distance S_W^* (calculated from pump speed and time of operation, (Figure 12), because in this case the wear curves for different speeds match into one. The course of the mass ratio m/m_N with respect to time is degressive. This phenomenon is due to the overlapping between rotor and stator present in the pumps used for the tests (diameter of the rotor larger than the stator opening width). This improves internal sealing. As wear increases, this overlapping compression drops, however. The total sliding distance is therefore prolonged as the rotational speed increases.

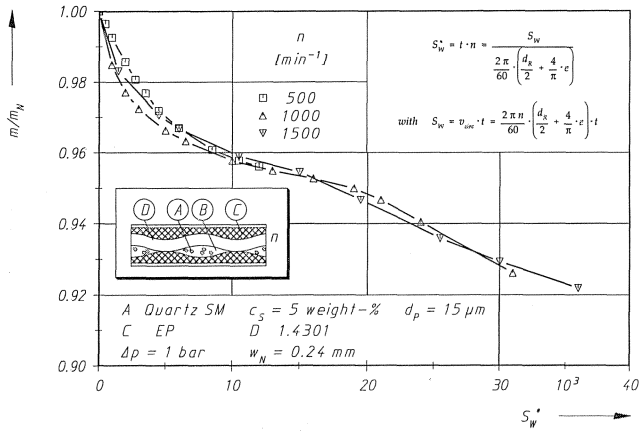

Figure 12. Influence of Pump Speed n on the Rotor Wear m/m_N (Plotted in Pump Speed as S_W^*).

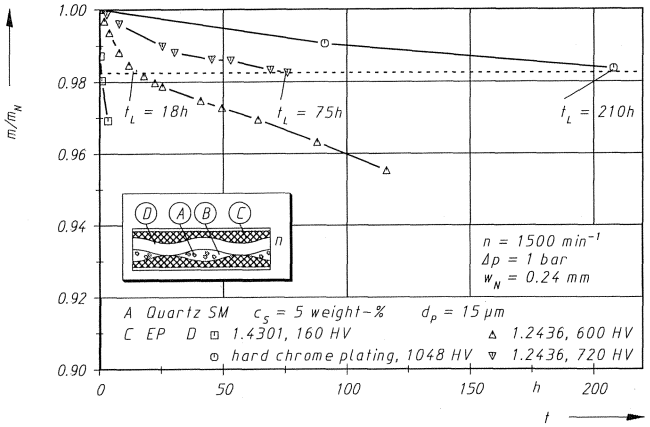

Figure 13. Influence of the Hardness of the Rotor Material $HV_{M,R}$ on the Rotor Wear m/m_N.

Hardness of the material of the rotor $HV_{M,R}$

With respect to the mass loss, the sequence of the materials used for the rotor parallels the sequence of increasing hardness (differing by a factor of 10 between steel type 1.2436 (Table 1) and a rotor surface with hard chrome plating (Figure 13). Again, the influence of the larger overlapping during the initial part of operation time is noticeable on the wear.

Table 1. Materials Considered within the Reported Investigations.

Group	Construction material	Hardness HV30
G1	X 5 CrNi 18 9 1.4301	160
G1	X 5 CrNiTiMoCu 21 8 Uranus 50	212
G1	X 10 CrNiMoTi 18 10 1.4571	160
G1	G-X 6 CrNiMoTi 18 10 1.4408	220
G1	X 20 Cr 13 1.4021	261
G1	X 2 CrNiMo 18 10 1.4404	325
G1	G-X 3 CrNiMoCu 24 6 9.4460 / 9.4460 DAS	310/380
G1	G-X 250 CrMo 15 3 NH 15.3	876
G2	X 22 CrNi 17 1.4057	570
G2	X 90 CrMoV 18 1.4112	630
G2	X 105 CrCoMo 18 10 1.4528	700
G2	X 210 CrW 12 1.2436	805 HV 10

Group	Construction material	Hardness HV30
G3	Ferro-Titanit U: 18Cr; 12 Ni; 34 TiC; 2 Mo; 1 Cu; rest Fe	535
G3	Ferro-Titanit S: 0,5 C; 19,5 Cr; 32 TiC; 2 Mo; 1 Cu; rest Fe	917
G3	Ferro-Titanit WFN: 13,5 Cr; 0,75 C; 0,4 Ni; 3 Mo; 0,8 Cu; 33 TiC; 1 Al; rest Fe	1150
G3	Stellit 20: 2,5 C; 33 Cr; 46,5 Co; 18 W	670
G4	Hard chromium plating	1048 HV 0.1
G4	Tungsten Carbide GT30: 85 WC; 15 Co	1150
G4	Tungsten Carbide GTD: 89,5 WC; 9,5 CrNi; 1 TiC + TaC	1530
G4	Si(SiC)	1500
G4	Cr_3C_2: 75 Cr_3C_2; 25 NiCr	930 HV 10
G4	Al_2O_3: 80 Al_2O_3; 20 ZrO_2	690 HV 10
G5	PVDF Polyvinylidenfluorid	
G5	FEP Perfluorethylenpropylen-Copolymer	
G5	EPDM Etylen-Propylen-Dien-Copolymer	
G5	UHMPE High Molecular Polyethylen	

Concentration of Solids c_S

The wear increases as the concentration of solids c_S in the suspension rises (Figure 14). Even low concentrations of solids cause significant wear on the rotor. The decrease in the rate of mass loss is attributable to processes of partial rejection of particles from the contact zone.

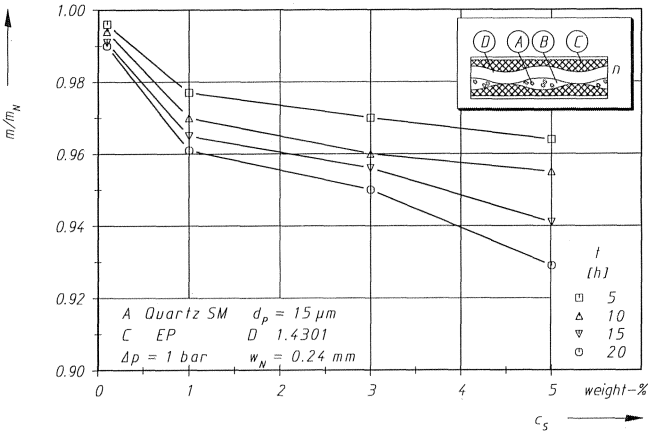

Figure 14. Influence of Particle Concentration c_S on the Rotor Wear m/m_N.

Summary

The experiments describe the influence of operational, material, and fluid parameters on the wear observed in a specific type of progressing cavity pump. The results, however, are not directly applicable towards different sizes or designs of pumps.

Tribometric Simulation by Means of the ROS-tribometer

The ROS-Tribometer offers a rather precise simulation of the kinematic conditions in a progressing cavity pump and meets the requirements for simulation closely approaching reality (Figure 10).

This type of tribometer is based on a division of the complex motion of the rotor of a progressing cavity pump into a rotational and an oscillatory component implemented on separately actuated samples [1].

The processes at the contact zone between the sample of metal (rotor) and the sample of elastomer (stator) along with the meshing area, correspond approximately to the conditions in the actual pump (Figure 15). In both cases, the particles are pulled into the area of contact between rotor and stator by the rotation of the rotor/rotating sample as it engages the elastic stator/elastomer sample. The three dimensional geometry of contact in a real pump is, however, duplicated by a quasi two-dimensional geometry of the samples only. Gaps between the transporting elements of the pump resulting in a change in the wear mechanisms are not considered.

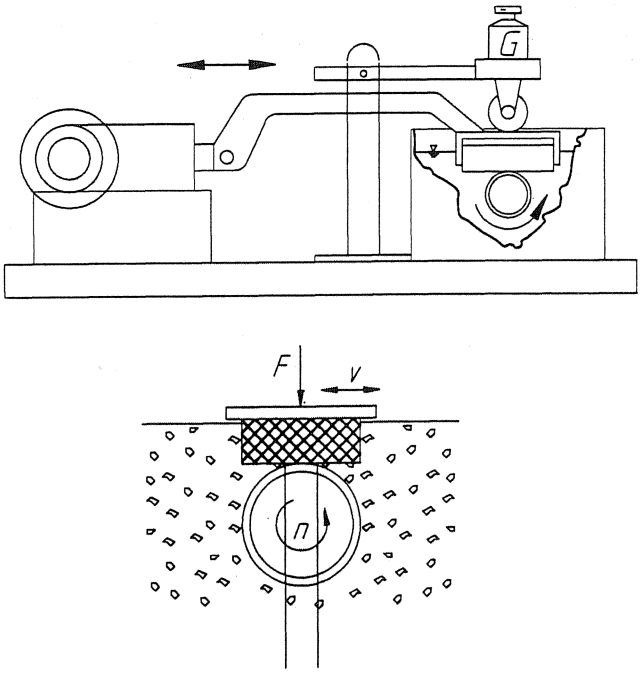

Figure 15. ROS-Tribometer: a) test rig; b) meshing situation.

To facilitate interpretation, the results of the effects of various parameters influencing the wear on the metal sample in the tribometer are depicted schematically only (details in Vetter and Wirth [1] and Wirth [6], but are based on a specific tribosystem (a suspension of quartz sand in water). The wear rates of the elastomer sample are commonly much lower (up to a factor of 6) (Figure 16).

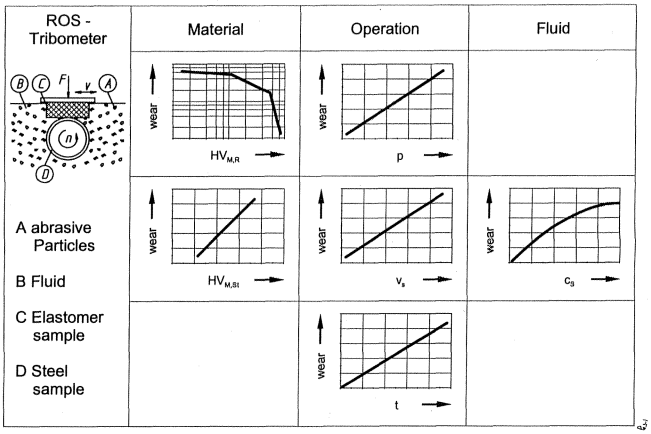

Figure 16. Wear Parameters (Schematical) of the ROS-Tribometer.

Hardness of the Material of the Rotor $HV_{M,R}$ (Rotational Sample)

The results correspond qualitatively to the results obtained on an actual pump. Plotting them on double logarithmic paper yields in sections a linear dependency of the wear rate on the hardness of the material. For a transition from soft chromium-nickel steel type 1.4301 (Table 1) to a hardened chromium steel type 1.2436, the wear rate drops by a factor of 20! For transition to hard chromium plated surfaces (HV = 1050), this factor rises approximately to a value of 40! [1]).

Hardness of the Elastomer $HV_{M,St}$ (Oscillatory Sample)

When increasing hardness of the elastomer samples, the wear rate rises approximately linearly. Lower hardness of the elastomer allows deeper imbedding of the solid particles into the surface of the elastomer and consequently results in a lower wear rate.

Contact Compression p

The overlapping of the progressing cavity pump and the contact compression in the tribometer being discussed are directly related. The influence of the contact compression on the wear rate is approximately linear.

Sliding Velocity v_s, Length of Period of Operation t

As the rotational speed of the pump, these parameters show a linear influence on the wear rate.

Concentration of Solid Particles c_S

Rising concentration of solids in the suspension results in increasing wear rates in the ROS-Tribometer. The influence of the particle concentration additionally increases for a rising speed. Most likely, more solid particles then enter the contact zone between rotor and stator.

For concentrations of the solid particles of 5.0 to 10 percent by weight the wear rate in this tribometer does not rise any more substantially. This phenomenon might be due to increasing rejection of the particles from the contact zone. The same basic response can be observed in field tests also.

Summary

For certain fluid properties, the simulation indicates parameters for optimization of the pump:

Reduction of the

- Positive interference w (Lowering of the contact compression)
- rotational speed n
- Hardness ratio R_H
- Hardness of the elastomer $HV_{M,St}$

Additionally, these tribometric data can be adapted to the conditions in the actual pump by appropriate computation.

A suitable approach is offered by Wirth [6].

$$\left(W_{m,t,A}\right)_P = \frac{\left(\frac{Wm}{\Delta t}\right)_P}{A_P}$$

$$\left(W_{m,t,A}\right)_{ROS,P} = \frac{\left(\frac{Wm}{\Delta t}\right)_{ROS}}{A_{ROS}} \cdot \frac{C_3 \cdot C_4}{C_1 \cdot C_2} \qquad (3)$$

The rates of loss of mass, $\{W_{m,t}\}_i$, are referred to the wear surface, A_i, the geometric data of the ROS-Tribometer are converted to the conditions in the pump by means of the factors C_1 (contact compression), C_2 (corrosion), C_3 (difference in magnitude) and C_4 (concentration of solids).

The comparison in Figure 17 shows field and tribometer test results for individual tribological conditions when applying the conversion algorithm based on Equation (3). The correlation is fair, but it should be noted, that actually not for all operating conditions the compression between rotor and stator can be evaluated. The example is based on an overlapping pump feature.

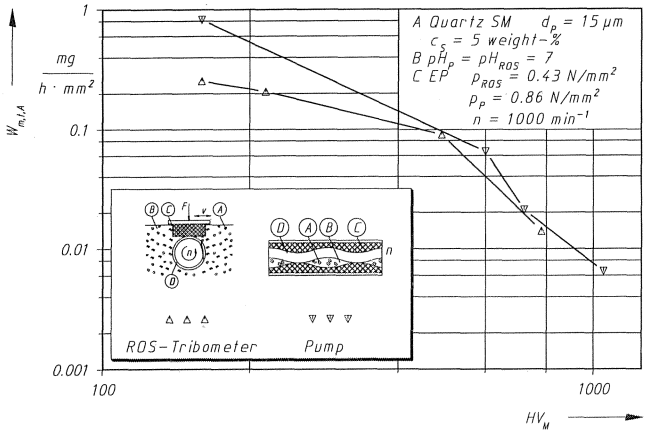

Figure 17. Comparing Wear Data from Field and ROS-Tribometer-Tests.

Tribometric Simulation by Means of the Miller-Tribometer

The Miller-Tribometer is used for simulation of systems with sliding wear pairing elastomers against steels or other hard materials. The mode of operation, the test procedure, and the evaluation of the results are well known (Figure 10) [7].

Evaluation of the results with respect to the resistance of materials against wear (in this tribosystem) yields the SAR-number, which can be converted into a wear rate (e.g., into the linear wear rate W_l [mm/a]).

Wear tests by means of the Miller-Tribometer yield a quantitative prognosis of the influences of the wear parameters only for the special tribosystem of the tribometer itself. If the tribometer is used in the standard mode of operation, not only the load, but also the geometric configuration, the kinematics, along with the concentration of solids in the slurry and the opposing elastomer material, are constant.

The parameter dependency shown in Figure 18, has been extracted from detailed investigations [1, 6, 8], refers to metal samples only, and is presented in a schematic form for convenient interpretation.

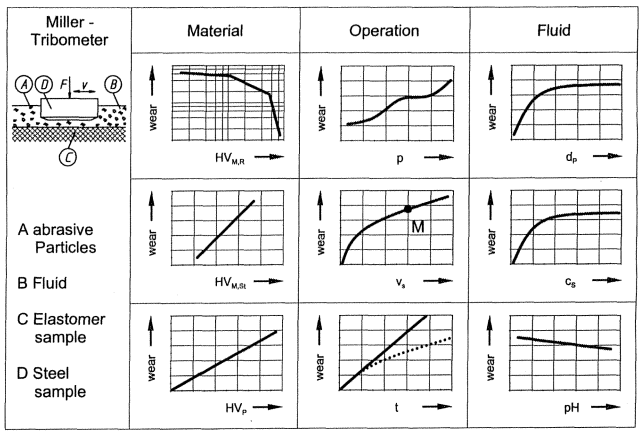

Figure 18. Wear Parameters (Schematic) of the Miller-Tribometer.

Hardness of the Rotor Material $HV_{M,R}$ (Sliding Sample)

Similarly to the field tests and the tests in the ROS-Tribometer, plotting the results on double logarithmic paper yields in sections a linear dependency of the wear rate on the hardness of the material. More details on this phenomenon will be mentioned in a later section.

Hardness of the Elastomer $HV_{M,St}$ (Opposing Surface)

The course of the wear rate *vs* the Shore-A hardness of the elastomer, roughly approximating a linear response, apparently results from the embedding of the particles into the elastomer. A different response with respect to wear for rigid, unelastic, slide ways (which are normally elastomer liners in the Miller-tribometer) is noteworthy.

Hardness of the Wear Particles HV_P

The rate of wear corresponds approximately linearly with the hardness (HV_P) of the particles. This influence is observed similarly in the tests in the field and in the ROS-Tribometer tests.

Contact Compression p

The loss of mass rate increases approximately linearly for a rising contact compression p.

Sliding Velocity v_S

Starting from the standard conditions (Figure 18, Point M), the special conditions for engagement in the Miller-Tribometer result in increasing, resp. decreasing loss of mass rates.

Influence of the Duration t of a Test Run

If the suspension is not changed (Figure 18, dotted characteristic), the characteristic for the loss of mass will become more and more flat, due to destruction of the particles. This effect will not be noticeable if exchanges of the suspension are provided (solid characteristic).

Particle Size d_P

Rising size of the particles generally results in an increased wear rate and a flatter course of the corresponding characteristic. Large particles no longer enter the zone of engagement, but are pushed along on the elastomer sliding way. For harder abrasive materials, the flatter part of the characteristic is shifted towards the range for larger particles (rolling motion of the particles in the area of engagement).

Concentration of Solids c_S

Quite similar to the conditions in the ROS-test, for medium size of the particles exceeding 100 µm, the concentration of solids has a significant influence up to concentrations of 10 percent by weight. The noticeable increase of the wear even low concentrations already indicates the effect of minor concentrations of solids (dirt!).

For smaller size of the particles ($d_P \approx 15\mu m$) the influence of the concentration is approximately linear (easy entry of the particles into the zone of engagement).

Corrosion (pH-Value)

If corrosion is superimposed to other conditions, the wear rate generally rises.

Summary and Comparison

The Miller-Tribometer, with sliding motion features, demonstrates very special dependencies on some parameters, which have to be taken into account during comparison of data. The results obtained by means of the ROS-Tribometer and the Miller-Tribometer are to some extent, mutually applicable [6]. With respect to the influence of the concentration of solids significant differences exist however (Figure 19). These differences result from the respective mode of engagement of the particles (ROS: oscillating motion, Miller: lifting of the probe at the end of the stroke).

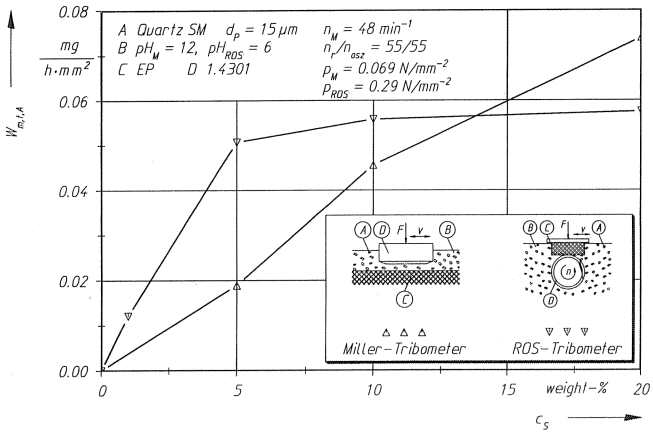

Figure 19. Comparing of Wear Data from Miller- and ROS-Tribometer- Tests.

The comparison of the two types of tribometers can be summarized in the following statements:

The Miller-Tribometer is well suited for voluminous studies of specific parameters and furnishes data for classification of materials in series, thus permitting optimatization of an actual pump. The ROS-Tribometer, on the other hand, provides much better simulation of the wear occurring in a pump for computation of approximate prognoses on the service life of a pump.

The investigations demonstrate the considerable chances the tribometric methods offer towards an increase of the service life of pumps in the presence of abrasive wear.

Tribosystems Predominantly Experiencing Jet Wear

Jet wear in pumps occurs predominantly subject to flows of fluid in narrow clearances (sealing gaps in centrifugal pumps and in rotary displacement pumps) and in flow ducts (impellers and housings of centrifugal pumps).

Jet Wear in Clearances

For optimal hydraulic efficiency, the leak volume through clearances has to be minimized by appropriate means. The two features of these clearances open for modification are the width and the length. A long, inclined clearance (Figure 6(b)) avoids orthogonal impact of the wear particles causing intensive wear (Figure 6(a)) and is, for example, well suited for centrifugal pumps operating with abrasive fluid, as this modification may reduce the wear rate by a factor of 10! [9, 10, 12].

The length of the clearances in rotary displacement pumps is largely determined by the pump design (Figure 6(c), Two Screw Pump). The width of the clearances is open only for optimization in most of the cases.

Methods of Quantitative Wear Prediction

As mentioned, field tests for comprehensive studies on parameters are uneconomical. An analysis of the jet wear in clearances can, however, be performed by tribologic simulation. The use of a jet tribometer represents an approach allowing an investigation of all influences: geometry of the clearance, principal properties of the fluid, operational conditions such as the velocity of the flow, the rotational speed, and the materials to be used.

Data exist already for some simple jet tribometers [8, 11, 12], which can be used to determine a sequence of materials allowing an optimization of the pump, with respect to the materials used (method of relative suitability).

The analysis of wear mechanisms in the tribosystem of concentric annular clearances requires an investigation of the particle motion relative to the surrounding walls.

The clearances are long, narrow gaps (ratio of length/width approximately 100), with turbulent flow. Parallel jet wear occurs, since the particles do not hit the walls at a defined angle. If a fraction of the coarse particles reaches the width of the gap, the jet wear becomes superimposed by sliding wear. Particles significantly larger than the clearance cannot cause any wear as they are rejected (Figure 8).

The following considerations cover jet wear, as it is present in finely grained suspensions. The radially fluctuating movements of the particles in turbulent flows have a dominant influence. The particles' motion due to the centrifugal acceleration, caused by the rotation of the inner cylinder, however, can be disregarded [12].

While motion results in axial grooving on the outer cylindrical surface, additional tangential grooves develop on the inner cylindrical surface (Figure 20(a)).

Since the surface of the outer cylinder does not rotate, axial grooving predominates there, and the wear rate is lower than the rate at the inner cylinder.

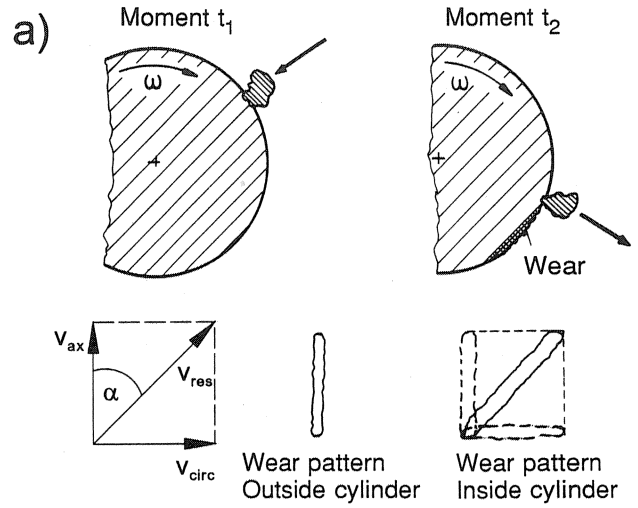

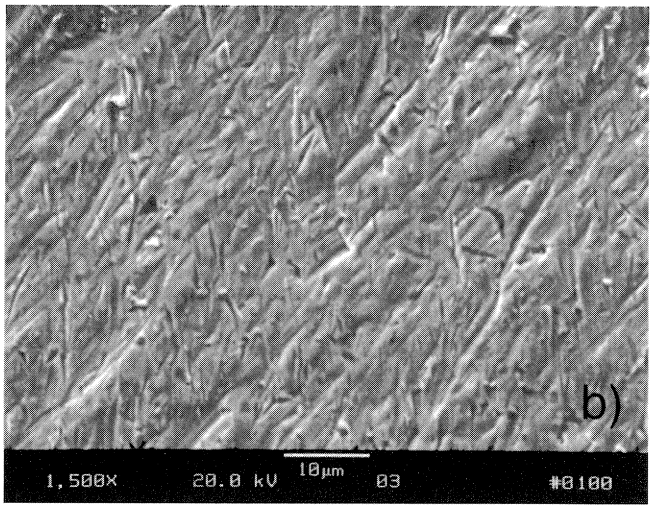

Figure 20. Influence of the Axial and Circumferential Speed on the Direction of Wear (Inner Cylinder).

The picture of a worn cylindrical sample of material (Figure 20(b)) shows the resulting vector of wear to be inclined against the flow (axial velocity component v_{ax}) by the angle α (circumferential velocity component v_{circ}).

Rotary Clearance Type Tribometer (Figure 21)

The configuration and the operational details have to be adapted to the specific application. The suspension enters the device at (1) and leaves it at (6). Together with the stator cylinder the inner cylinder (3) rotating on the shaft (8) forms an annular gap (4). The outer cylinder (2), along with the inner cylinder (3), can be manufactured as samples of a specific material. To prevent falsification of the results by wear occurring at the faces of the specimen, these are protected by covers made of hard metal.

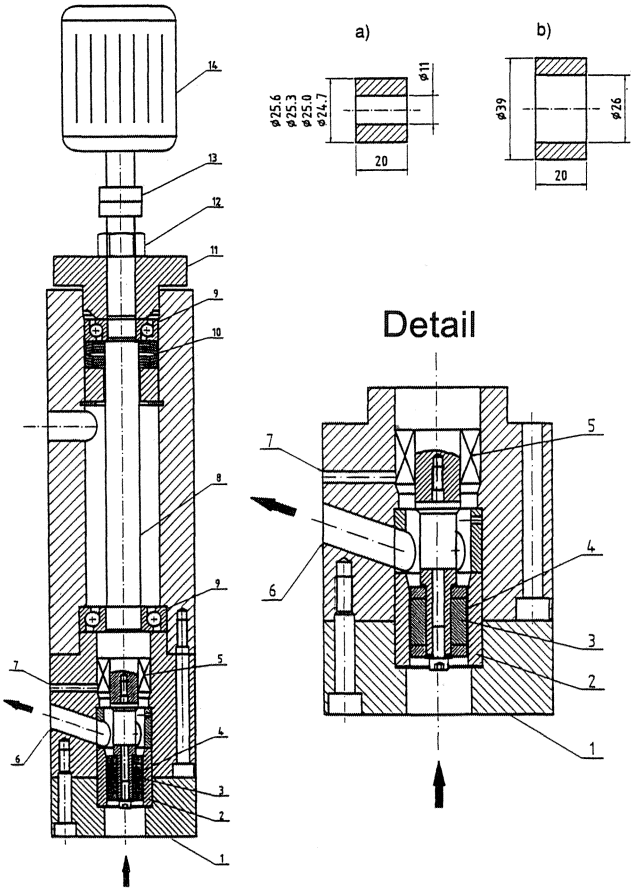

Figure 21. Rotary Clearance Tribometer.

The rotary clearance type tribometer is integrated into a test loop for the suspension, comprising a reservoir with a stirring device, a pump and a flowmeter.

Axial and Circumferential Velocity

The linear wear rate at the rotating cylinder is additively composed by the contributions of axial (v_{ax}) and circumferential velocity (v_{circ}) (Figure 22).

$$W_{l,tot} = W_{l,ax} + W_{l,circ} \tag{4}$$

At the outer cylinder almost no influence of the rotational speed exists.

$$W_{l,tot} = W_{l,ax} \tag{5}$$

Quantitatively, the correlation between the wear rate and the axial, respectively, circumferential velocity can be expressed by a power law that comprises the vectorial resultant v_{res} composed of the velocity contributions v_{ax} and v_{circ} (Figure 23).

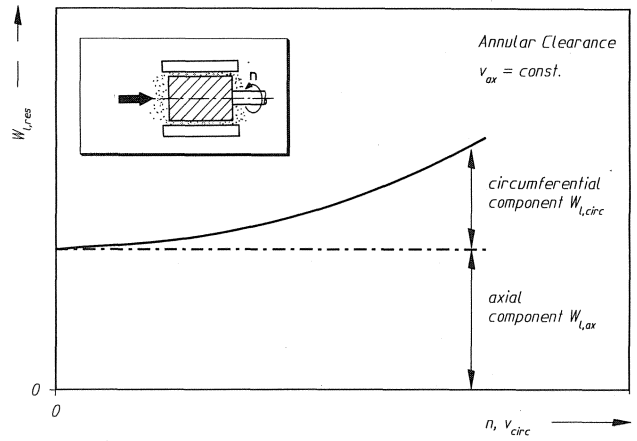

Figure 22. Influence of the Axial and Circumferential Speed on the Total Wear Rate (Inner Cylinder).

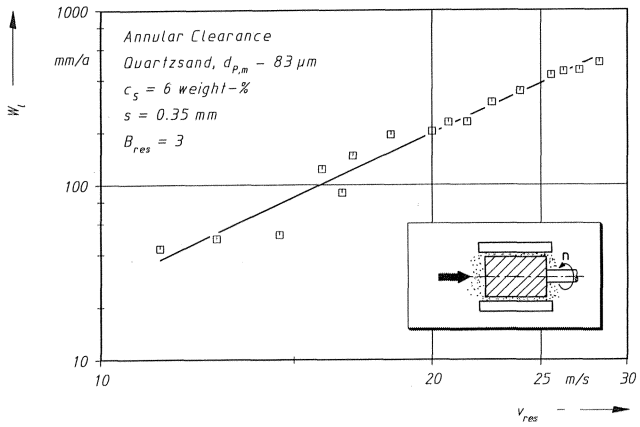

Figure 23. Linear Wear Rate Vs *Resulting Velocity.*

$$W_l \sim v_{res}^{B_{res}} \Rightarrow W_l \sim \left(\sqrt{v_{ax}^2 + v_{circ}^2}\right)^3 \tag{6}$$

Illustratively this means: For high flow velocities, e.g., two screw pumps, the resulting vector of wear deviates marginally from the axial component only. The circumferential component has just a minor influence.

For low flow velocities, e.g., centrifugal pumps, the tangential component of the wear, and accordingly, the circumferential velocity, contribute a substantial share to the total wear rate.

At the outer cylinder, the power law customarily used for jet wear can be applied (no influence of the rotation of the inner cylinder).

$$W_l \sim v_{ax}^{B_{ax}} \Rightarrow W_l \sim v_{ax}^3 \tag{7}$$

Width of the Gap

Commonly the clearances in the seals are selected as small as possible to minimize the slip flows. At a constant speed of the flow, the linear rate of wear initially decreases substantially as the width of the clearance increases, since for wider clearances the probability for a particle to hit a wall (expressed by the characteristic number C_I) is less. After a minimum, the linear wear rate rises for even wider clearances only by a small amount (Figure 24). For constant velocity of flow, the volume flow rises, however, according to the increase in the cross sectional area, admitting more wear particles into the gap. Both effects are superimposed to create the response just described.

$$C_1 \sim (0.65...1) \cdot s^{-(1.1...1.4)} \quad (8)$$

$$W_1 \sim C_1 \cdot Q \quad \text{für} \quad \upsilon = \text{const.} \quad (9)$$

$$\Rightarrow \quad W_1 \sim (0.65...1) \cdot s^{-(1.1...1.4)} \cdot Q \quad (10)$$

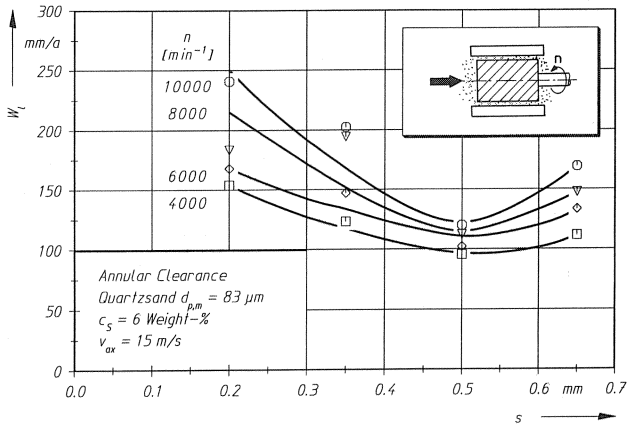

Figure 24. Linear Rate of Wear Related to the Width of the Gap for Various Rotational Speeds (Inner Cylinder).

Transition from Jet to Sliding Wear

If the fluid contains particles of coarse size, these particles may jam themselves into the gap, causing sliding wear at a high rate. The influence of the size of the particles will be explained with an example (width s = 0.2 mm, sand/water suspension, mean particle size $d_{P,m}$ = 186 µm, share of particles exceeding 0.2 mm in size by weight approximately 35 percent):

The rotating inner cylinder is shown in Figure 25: While the share of fine grain particles ($d_P < s$) causes jet wear in the direction of the flow (position 1), the share of coarse grains ($d_P \approx s$) becomes jammed between the housing and the inner cylinder, causing deep wear marks extending in the circumferential direction, due to the rotation of the inner cylinder (position 2).

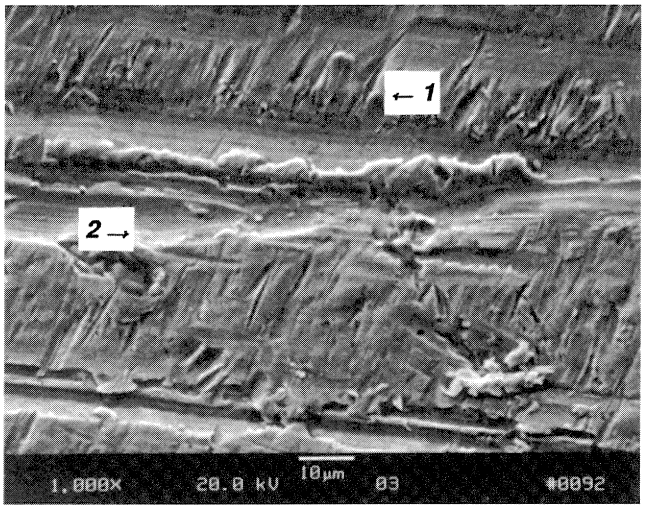

Figure 25. Wear in the Transitional Area between Jet Wear and Sliding Wear: 1) jet wear; 2) sliding wear.

These findings have the following consequences for the actual design and operation of pumps:

In two screw pumps, the high rates of wear will occur for the mean size of the particles in the fluid matching the range of the width of the gap. If the spectrum of size of the particles comprises very small particles only, a substantially lower loss of material can be expected due to the reasons just explained. If a large part of the spectrum of particles comprises particles exceeding the width of the gap in size, such particles cannot enter and pass the gap (rejection effect) and may get transported from the suction to the pressure side within the transport chambers. For hydraulical and tribological reasons the design of pumps should, therefore, employ gaps of optimized design with minimal widths.

The inside of the pump housing can be coated uniformly with a durable hard material. The core of the screws has to be ductile, as the screws experience flexing loads due to the pressure gradient from the suction towards the discharge side. Layers of hard materials should, therefore, be applied to the circumferential rims including the edges only.

For the design of centrifugal pumps, the composition of the spectrum of particles actually showing at the gap of the seal during operation should be estimated (centrifugal forces). The selection of an inclined clearance and the design of the outer wall of the gap as a replaceable hard (Si-SiC hard metal coatings) split ring are means of the design and the selection of materials for minimizing wear. Widening of the sealing clearance may be compensated by an axial shift of the rotor possible within a certain range. Operation of a pump in the transitional range from jet to sliding wear should be avoided. Otherwise, an armoring coating of hard material resisting the wear should be applied in the area of the gap.

Concentration of Solids c_S

For low concentrations of solids in the fluid ($c_S < 5$ weight-percent) the rise of the rate of wear is approximately linear. For growing concentrations the wear rate takes a slightly degressive course. The 'saturation effect' noticeable for higher concentrations may be attributable to mutual collisions of particles or to the influence of large shear forces in the gap.

Size of the Particles d_P

Across the range investigated the loss of material increases approximately linearly with the size of the particles. The dependency of the loss of material on the size of the particles may, however, vary for different concentration of solids and sizes of the particles. It is, therefore, advisable to use the genuine fluid for the tribometric simulation or to make efforts to match as closely as possible the model fluid with the genuine fluid.

Summary and Evaluation

Rotary clearance type tribometers permit good simulation for wear in clearances and allow easy analysis of the parameters sensitivity. The true composition of the fluid flowing through the gap in a pump should be known and be duplicated as close as possible.

Jet Wear in Flow Ducts

Hydroabrasive wear is caused by rapid flows through ducts in pumps, e.g., on the impellers of centrifugal pumps. In such pumps, particles in the fluid are accelerated by rotational and centrifugal forces. Because of their specific density, the particles hit the surrounding walls of the pump and wear results (Figure 26 [13]). The principal mechanisms of wear are:

- During deflection of the entering flow from axial into the radial direction, the particles hit the cover of the rotor due to their inertia (position IV).

• At the entrance of the duct, the flow hits the leading edges of the blades and flows around them (position I).

• During passage of the flow through the rotor duct, the particles hit the blades of the rotor, particularly on the pressure side (position II).

• The exit edges of the blades are particularly endangered, since eddy flows may develop in the areas where the flow departs from the blades (position III).

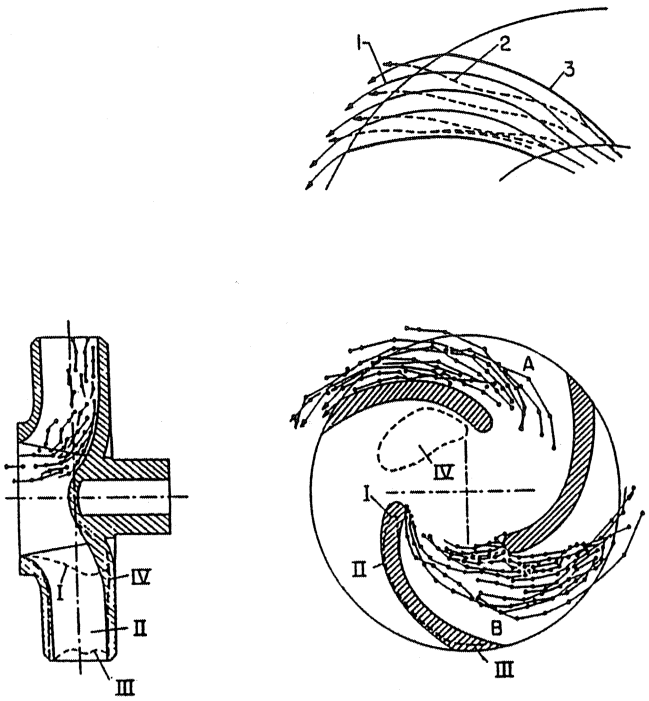

Figure 26. Paths of Particles and Areas of Maximum Wear in Centrifugal Pumps [13].

As the conditions of the flow are quite complex, the paths of the particles and accordingly, the local collisions of the particles with the walls cannot be determined and a quantitative prediction of the wear based on tribometric simulation is hardly possible. So far, wear prediction is limited and based on qualitative tribometric simulation only.

Methods of Qualitative Wear Prediction

Acquisition of the tendencies of wear influencing parameters, such as the velocity of the flow, the angle of attack, the concentration of solids in the slurry and the size, material and shape of the particles is feasible. The determination of the relative suitability, particularly of the materials, is possible. These evaluations cannot supply quantitative information on the wear rates occurring in the actual tribosystem of a pump in the field, however.

Jet wear tribometers are used for tribometric simulation [12], which are convenient to operate and require a simple configuration of the samples. In an orthogonal jet tribometer (Figure 27(a)) the flow of suspension is concentrated and defined by means of an orifice made of hard metal (1), subsequently hits the sample of material orthogonally (2) and leaves the chamber via the discharge channel in the housing (4). In a parallel jet tribometer, the suspension passes in a parallel flow through the channel through the sample (7). Orifices made of hard metal (1) protect the intake and discharge edges of the channel against wear. Serial passing of the suspension through two samples (Figure 27(a)) permits the simultaneous acquisition of two sets of results.

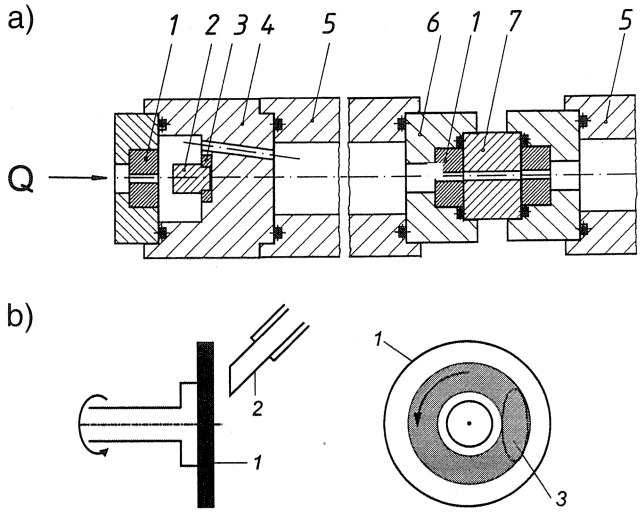

Figure 27. Jet Wear Tribometer: a) orthogonal jet/parallel jet tribometer; b)jet tribometer for investigation of the dependency of the rate of wear on the jet angle.

For investigation of jet wear with respect to the angle of attack of the suspension (Figure 27(b)) [14], the jet of suspension is directed on the sample of material (1) at a defined, but variable angle and at constant speed through a jet nozzle (2). To achieve a uniform pattern of wear (3) the sample rotates slowly around its axis. Jet tribometers integrated into closed loops of suspensions parameters allow studies.

Velocity of the Flow v

On metals, the wear observed rises approximately by the third power, with flow velocity for parallel jet wear, and by a power of 3.5 for orthogonal jet wear. This correlates well with theory.

$$W_1 \sim v^{B(\alpha)} \qquad B(\alpha) = 3 - 3.5 \tag{11}$$

$$W_1 \sim E_{kin,\text{single particle}} \qquad E_{kin} = \tfrac{1}{2} \cdot m_P \cdot v_P^2 \qquad (B = 2) \tag{12}$$

$$W_1 \sim \frac{\text{number of particles}}{\text{time period}} \cdot \frac{\Sigma m_P}{\Delta t} \sim v_P \qquad (B = 1)$$

For handling of corrosive fluids, coating of pump components with plastics, e.g., polyethylene, is advisable. For low flow velocities some plastic materials exhibit more or comparable durability against wear than austenitic and austenitic/ferritic steels. For higher flow velocities, the durability of plastics drops and the wear rate rises relatively. Increases of the wear by a power of 4 and up to 4.5 with flow velocity have been observed (Figure 28). For larger flow velocities the advantage of plastic materials disappears (Figure 29, extracted from Figure 28).

Since the wear rises exponentially with the flow velocity, regardless of the material selected for the rotor, efforts should be made to keep the flow velocity as low as possibly. Optionally, the flow guiding parts of pumps can be made of wear resistant, suitable materials.

Angle of Attack α

As seen, the surfaces of the impeller are hit by the particles at various angles, depending on the specific locality. In the face of the dependency of the wear rate on the angle of attack, the ductility of

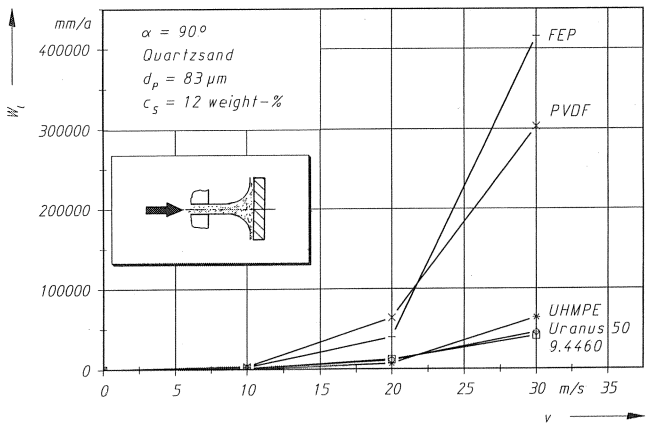

Figure 28. Wear Vs *Flow Velocity for Various Materials.*

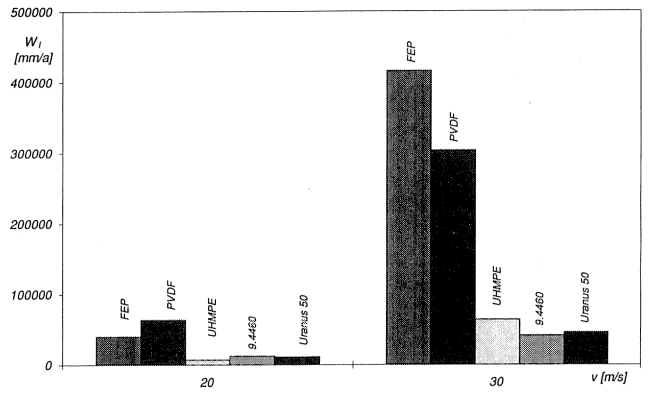

Figure 29. Special Wear Characteristics based on the Flow Velocity.

the rotor material represents an important criterion. The influence of the angle of attack is attributable to the energy of the particle attack, which is represented in Figure 30 by the energetic wear rate.

$$W_E = \frac{\Delta m}{\rho \cdot E_{kin}} \tag{13}$$

$$E_{kin} = \frac{1}{2} \cdot M_s \cdot \upsilon^2 \tag{14}$$

Δ m is the mass loss and M_S the total particle mass within observation time with flow velocity v and material density ρ.

Brittle, nonmetallic materials show a monotonous increase of the rate of wear for rising angles of attack (Figure 30, Al_2O_3).

For jet angles ranging approximately between 30 and 60 degrees, ductile materials show a maximum rate of wear (9.4460). Harder and lesser ductile metallic materials demonstrate the maximum at larger angles and much lower wear rates (Figure 30, NH).

Thanks to their elasticity, elastomers exhibit good resistance against wear with orthogonal flow (at least for low flow velocities). There is a typical influence of the angle of attack, which is different for various plastic types (Figure 30, EPDM, UHMPE).

There are the following consequences for the pumps:

• The pump should be operated at the point of highest efficiency with a minimum of losses due to impact and eddy flow effects resulting in small angles of attack.

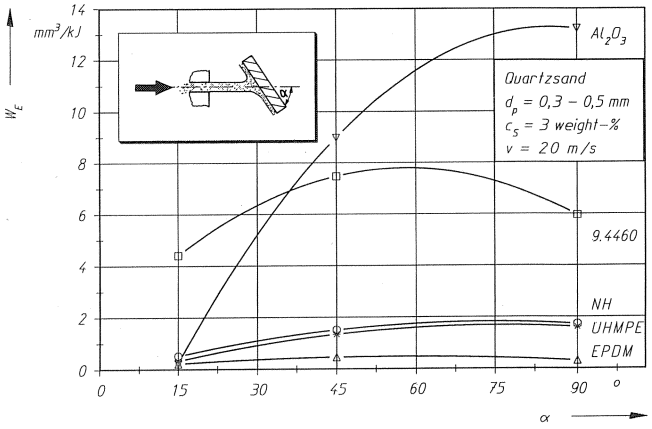

Figure 30. Energetic Wear Rate Vs *Angle of Attack.*

• In order to avoid large jet angles, the deflection of the suspension in the rotor from the axial into the radial direction should occur at a moderate and uniform rate.

• Locations strongly exposed to wear should be plated with hard metals or lined with suitable elastomers.

Concentration of Solids c_S and of the Particle Size d_P

The influence of concentration and of particle size corresponds for flow ducts in a pump well with the dependencies determined with the clearance type tribometers. At least for low concentrations and small particles, the wear rate rises approximately linearly for increasing concentration and particle size. For optimal simulation, the original fluid or a comparable model fluid should be used.

MATERIALS

The dominant parameter for the solution of most of the wear problems is the material selection. Out of the large number of the physical and chemical parameters, in the following section some aspects about the hardness influence are explained.

Characterization of Pump Materials

As design and hydraulic parameters are representing rather limited means to reduce wear, it is important to understand the material characteristics. In Table 1, the relevant selections out of a range of available materials have been divided into five groups:

• *Group G1: Ferritic and austenitic forged and cast alloys.* Applied in pumps due to good corrosion resistance and ductility. As hardness is low (HV < 500), the suitability for hydroabrasive wear is restricted.

• *Group G2: Martensitic-carbidic forged or cast alloys.* Hardness can be increased (HV > 500) by heat treatment, but corrosion resistance and ductility are reduced. For a number of applications these materials are a good choice for hydroabrasive low corrosion attack.

• *Group G3: Special alloys with hard carbidic inclusions.* The basic matrix contains hard carbidic inclusions, either by precipitation or by external implementation as particles. The hard particles or phase areas represent together with the basic material matrix a reinforced structure against wear attack. These materials are available as castings or welded resp. sprayed coatings. Hardness is high (500 < HV < 1000).

• *Group G4: Hard metals and ceramics.* Hard metals are mainly based on carbide particles embedded within a metallic matrix. They can be used either as sintered parts or as sprayed coatings. High wear resistance is paired with brittleness and difficult machining (HV > 1000).

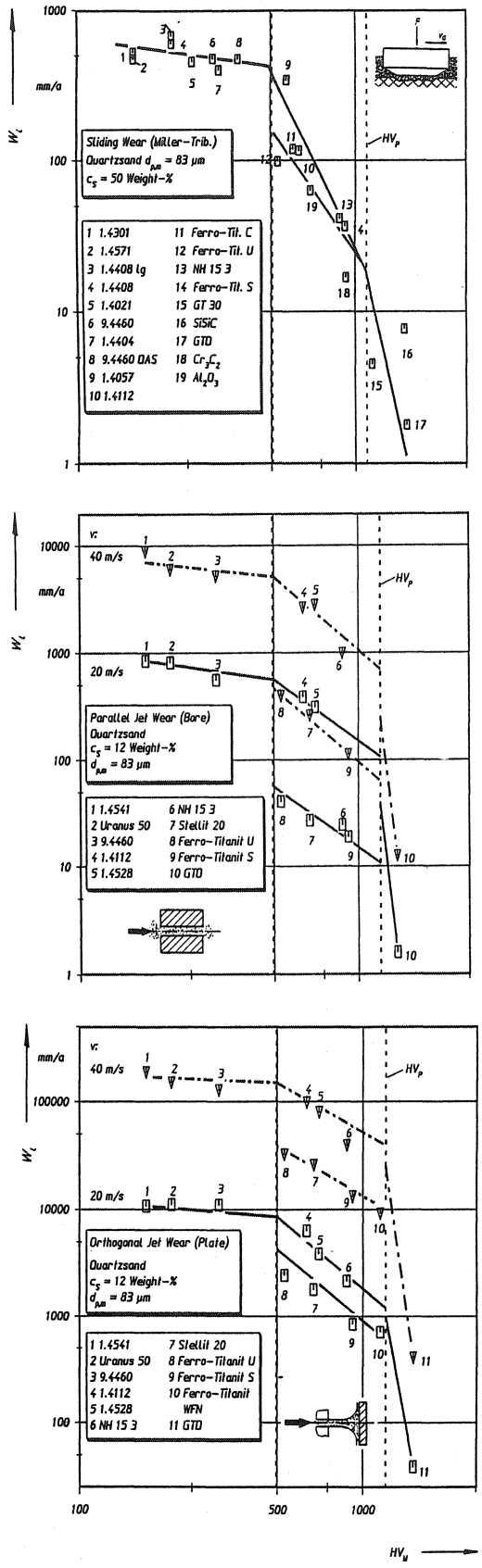

Figure 31. Linear Wear Rate Related to the Hardness of the Material: a) sliding wear; b) parallel jet wear (bore); c) orthogonal jet wear.

• *Group G5: Plastomers and elastomers.* Corrosion and wear resistance make these materials attractive for lining or coating of pump components.

Material Hardness and Wear Resistance

For most of the materials, except of the plastic type materials, the hardness/wear correlation is definite. For comparable tribological conditions that with sliding and orthogonal, respectively, parallel jet wear very similar characteristics of the material groups G1 - G4 are shown in Figure 31.

Group G1 (HV < 500): Increased hardness does not reduce wear rate much, as the tribological system in on the high wear level ($R_H > 1$).

Group G2 (HV > 500): Increased hardness shows a stronger influence on wear rate. Double hardness yields sliding wear reduction by a factor 20 to 40 and jet wear reduction by factor 2.0 to 5.0.

Group G3 (HV > 500): Alloys with carbide inclusions demonstrate at nominally equal hardness improved wear resistance, as local hard inclusions act as a shield.

Group G4 (HV > 1200): Due to the transition of the tribological system from the high to the low wear level ($R_H \leq 1$), the wear rates are reduced substantially by factor 100 and more.

The similarity of tribometric test results is clearly demonstrated in Figure 31 with respect to the relative suitability of materials. This is also true for the results of the rotary clearance tribometer (Figure 32). From Figure 31(b) and (c) yield the great difference in wear rate between parallel ($\alpha = 0$) and orthogonal ($\alpha = 90$ degrees) flow direction (Factor 10 and more!).

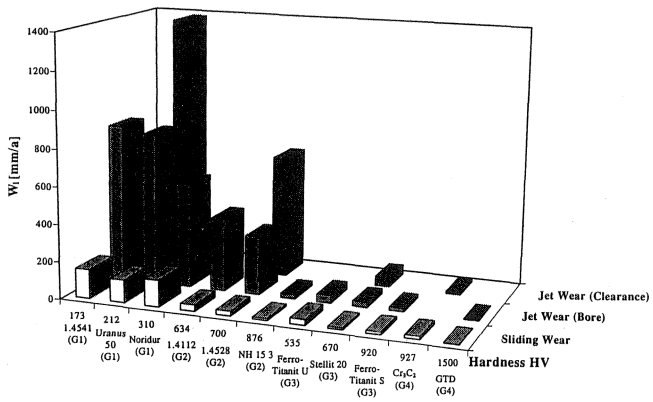

Figure 32. Relative Material Suitability based on Different Tribometric Data.

As the reported results are related to a definite tribosystem (particle characterisation, concentration, hardness etc.), they are, therefore, not directly transformable to other conditions.

Material Suitability and Optimization

There are some possibilities to improve material hardness (HV ≈ 800) by various (surface) hardening processes (thermal treatment, nitration etc.). A further step is the implementation of hard particles, e.g., carbides like TC, Cr_3C_2, into a metallic matrix (CoCr, NiCr). The shielding mechanism for sliding and jet wear is demonstrated in Figure 33.

It is possible for certain types of stainless cast steels to control the precipitation of hard carbides by thermal treatment in a manner that an improvement of wear resistance results due to the shielding effects mentioned previously.

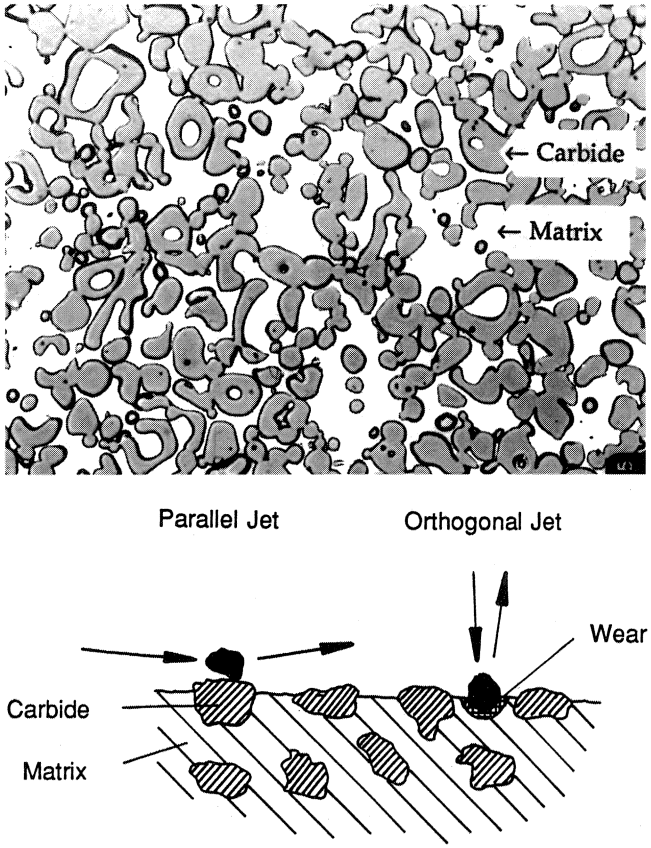

Figure 33. Protective Effect of Carbide Deposits in Cases of Jet Wear.

CONCLUSIONS

Various pump types demonstrate characteristic tribological systems at definite locations, dominatingly based on sliding or jet wear attack. Evidently for many pump features, it is feasible to develop tribometers that simulate the individual tribological conditions well and allow quantitative wear prediction and endurance estimations. This is especially true for sliding and parallel jet wear attacks as they commonly exist in various types of displacement pumps and annular clearance seals in general.

The application of tribometric tests for quantitative jet wear prediction in flow ducts of centrifugal pumps yields difficult, as the evaluation of the particle paths and energy relative to the wearing pump components wall is not solved satisfactorily.The application of the method of relative suitability for the selection of the optimum pump material appears very efficient for sliding and jet wear attacks.

The tribometric approach to improve pump life during abrasive wear attack turns out to represent an efficient tool.

NOMENCLATURE

Symbol	*Unit*	*Designation*
α	°	angle
ρ	kg/m^3	density
ϑ	°C	temperature
η	Pas	viscosity
ω	1/s	angular velocity
A	m^2	area
C_i	-	constant
C_I	-	impact constant
c_S	kg/m^3	concentration of the slurry
d_P	mm	particle diameter
$d_{P,m}$	mm	average particle diameter
d_R	mm	rotor diameter
E_{kin}	W	kinetic energy
e	mm	eccentricity
F	N	force
HV_M	-	hardness of sample material
$HV_{M,R}$	-	hardness of rotor material
$HV_{M,St}$	-	hardness of stator material
HV_P	-	hardness of particles
HV_S	-	hardness of wearing surface
M_R	-	meshing ratio
M_S	kg	total mass of solids
MN	-	Miller-number
m	kg	mass of pump rotor
m_N	kg	mass of new pump rotor
m_P	kg	mass of particle
Δm	kg	mass loss
n	min^{-1}	speed
n_M	min^{-1}	speed Miller-Tribometer
n_r	min^{-1}	speed of the rotational drive of the ROS-Tribometer
n_{osc}	min^{-1}	stroke frequency of the oscillatory drive of the ROS-Tribometer
n_r	min^{-1}	speed of the rotational drive of the ROS-Tribometer
p	N/mm^2	contact compression
p_M	N/mm^2	contact compression in the Miller-Tribometer
p_{ROS}	N/mm^2	contact compression in the ROS-Tribometer
pH	-	pH-value
pH_M	-	pH-value in the Miller-Tribometer
pH_{ROS}	-	pH-value in the ROS-Tribometer
Δp	bar	pressure differential
Q	m^3/h	volume flow
R_H	-	hardness ratio
SAR	-	SAR-number
S_W	m	wear path
S_W^*	-	wear path
s	mm	gap width
t	h	time period
t_L	h	life time
t_M	s	meshing time
t_{tot}	s	time period

t	s	time period
v	m/s	velocity
v_{ax}	m/s	axial velocity
v_c	m/s	contact velocity
v_{circ}	m/s	circumferential velocity
v_P	m/s	velocity of particle
v_{res}	m/s	resulting velocity
v_s	m/s	sliding velocity
W_E	mm^3/kJ	energetic wear rate
W_l	mm/a	linear rate of loss of mass
$W_{l,ax}$	mm/a	linear rate of loss of mass due to axial velocity
$W_{l,circ}$	mm/a	linear rate of loss of mass due to circumferential velocity
$W_{l,tot}$	mm/a	total linear rate of loss of mass
W_m	mg	loss of mass
$W_{m,t}$	mg/h	rate of loss of mass
$W_{m,t,A}$	$mg/(h \cdot m^2)$	rate of loss of mass per area
$\{W_{m,t,A}\}_P$	$mg/(h \cdot m^2)$	rate of loss of mass per area, pump
$\{W_{m,t,A}\}_{ROS,P}$	$mg/(h \cdot m^2)$	rate of loss of mass per area, ROS-tribometer, upscaled to pump
w	mm	overlapping
w_N	mm	overlapping of new pump

REFERENCES

1. Vetter, G. and Wirth, W., "Understand Progressing Cavity Pumps Characteristics and Avoid Abrasive Wear," *Proceedings of the Twelfth International Pump Users Symposium,* Turbomachinery Laboratory, Texas A&M University, College Station, Texas, pp. 47-59 (1989).
2. Vetter, G., Thiel, E. and Störk, U., "Reciprocating Pump Valve Design," *Proceedings of the Sixth International Pump Users Symposium,* Turbomachinery Laboratory, Texas A&M University, College Station, Texas, pp. 39-52 (1989).
3. Uetz, H., "Abrasion and Erosion," Carl Hanser Verlag (1981).
4. Vetter, G, "Watch Characteristics of Metering Pumps for Good Accuracy," World Pumps, pp. 63-69 (1989).
5. Vetter, G.and Störk, U., Zum Verschleiß selbsttätiger Ventile oszillierender Verdrängerpumpen durch abrasive Suspensionen, Konstruktion 41, Nr. 1 pp. 3-12, Nr. 2 pp. 67-72 (1989).
6. Wirth, W., Zur hydraulischen and tribometrischen Simulation von Exzenterschneckenpumpen, Dissertation, Universität Erlangen-Nürnberg (1993).
7. N.N., ASTMG 2.3, Standard Test Method for Slurry Abrasivity Determination, 11-16-80 (1980).
8. Vetter, G. and Klotzbücher, G., Einige tribologische Grundlagenuntersuchungen zum abrasiven Gleit- und Strahlverschleiß von Pumpenwerkstoffen, Konstruktion 45, (11), pp. 371-378 (1993).
9. Radke, M., Siekmann, H. and Taenzer, L., Neue konstruktive Entwicklungen für Kreiselpumpen in Rauchgasentschwefelungsanlagen, Konstruktion *42,* (2), pp. 53-60 (1990).
10. Lünzmann, H. and Kosyna, G., Untersuchungen an Kreiselpumpen mit Schrägspalt Preprint, Pumpentagung Karlsruhe (1988).
11. Vetter, G. and Kießling, R., Verschleißverhalten von Pumpenwerkstoffen bei hydroabrasiver Strahlbeanspruchung, Konstruktion *47,* (6), pp. 186-190 (1995).
12. Kießling, R., Zur Modellierung und Simulation des hydroabrasiven Verschleißes ringförmiger Strömungsspalte, Dissertation, Universität Erlangen-Nürnberg (1994).
13. Shook, C.A. and Roco, M.C., *Particle Flow - Principles and Practise,* Boston: Butterworth-Heinemann (1991).
14. Förster, B., Der Einfluß der Verschleißparameter auf die Verschleißmechnismen von unterschiedlichen Werkstoffgruppen, Diplomarbeit, Lehrstuhl für Apparatetechnik und Chemiemaschinenbau, Universität Erlangen-Nürnberg (1994).